

A non-symmetric pillar[5]arene-based selective anion receptor for fluoride

Guocan Yu,^a Zibin Zhang,^a Chengyou Han,^a Min Xue,^a Qizhong Zhou,^{*b} and Feihe Huang^{*a}

Department of Chemistry, Zhejiang University, Hangzhou 310027, P. R. China, and

Department of Chemistry, Taizhou University, Taizhou 317000, P. R. China

Fax: +86-571-8795-1895; Tel: +86-571-8795-3189; Email address: fhuang@zju.edu.cn.

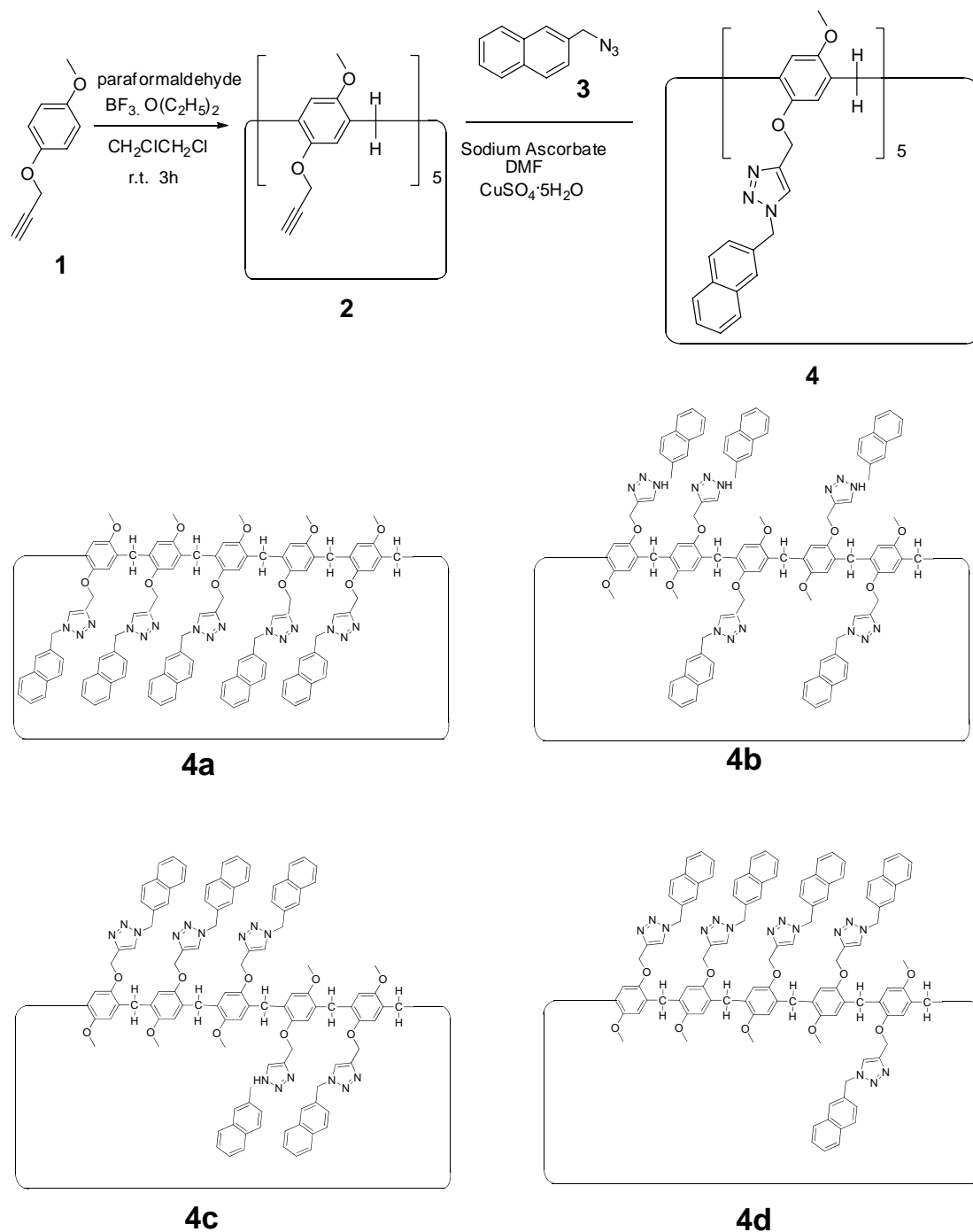
Electronic Supplementary Information

1. <i>Materials and methods</i>	S2
2. <i>Syntheses of 4a and the model compound 5</i>	S3
3. <i>Determination of association constants for the complexes between 4a and anions and between 5 and TBAF by fluorescence titration experiments</i>	S9
4. <i>Partial ¹H NMR spectra of model compound 5 and a mixture of 5 and tetrabutylammonium fluoride</i>	S20
5. <i>Partial ¹H NMR spectra recorded in acetone-d₆ during the titration of 4a with TBAX</i>	S20
6. <i>¹⁹F NMR spectra of 4a and a mixture of 4a and tetrabutylammonium fluoride</i>	S21
7. <i>¹H-¹H NOESY spectra of 4a and 4a in the presence of 2 equiv of TBAF in acetone-d₆ at 298 K</i>	S21
8. <i>Partial ¹H NMR spectra of mixtures of 4a and tetrabutylammonium salts with different anions</i>	S22
9. <i>The energy-minimized structure of 4a and 4a⊃F⁻</i>	S24

1. Materials and methods

Hydroquinone, propargyl bromide solution, boron trifluoride ethyl ether complex, 2-bromomethylnaphthalene, sodium azide and 4-methoxyphenol were reagent grade and used as received. Solvents were either employed as purchased or dried according to procedures described in the literature. ^1H NMR spectra were collected on a Varian Unity INOVA-400 spectrometer with internal standard TMS. ^{13}C NMR spectra were recorded on a Bruker Advance DMX-500 spectrometry at 125 MHz. Mass spectra were obtained on a Bruker Esquire 3000 plus mass spectrometer (Bruker-Franzen Analytik GmbH Bremen, Germany) equipped with an ESI interface and an ion trap analyzer. HRMS were obtained on a WATERS GCT Premier mass spectrometer. The fluorescence titration experiments were conducted on a RF-5301 spectrofluorophotometer (Shimadzu Corporation, Japan). The melting points were collected on a SHPSIC WRS-2 automatic melting point apparatus.

2. Syntheses of **4a** and the model compound **5**



To a solution of **1**^{SI} (4.02 g, 24.8 mmol) in 1,2-dichloroethane (about 150 mL), paraformaldehyde (0.74 g, 25 mmol) was added under nitrogen atmosphere. Then boron trifluoride diethyl etherate (10 mL) was added to the solution and the mixture was stirred at room temperature for 3 h. Water (10 mL) was added to quench the reaction. The mixture was filtered and the solvent was removed, the residue was dissolved in dichloromethane. The organic layer was dried over anhydrous Na_2SO_4 and evaporated to afford the crude product, which was isolated by flash column chromatography using ethyl acetate/petroleum ether (1:5) to give **2** as a white solid (2.21 g, 51%). Compound **2** is a non-symmetric pillar[5]arene and has four constitutional isomers. However, these isomers could not be separated here. Therefore, compound **2** was used in the next step without further separation.

Compound **3**^{S2} (7.51 g, 41.0 mmol), copper sulfate pentahydrate (30.0 mg, 0.120 mmol) and sodium ascorbate (225 mg, 1.60 mmol) were added to a solution of **2** (3.57 g, 4.10 mmol) in *N,N*-dimethylformamide (25.0 mL). The mixture was heated in a three-necked flask under nitrogen atmosphere at 90 °C for 1 d. The reaction mixture was diluted with ethyl acetate (30 mL) and washed with water (5 × 5 mL). The organic phase was dried over magnesium sulfate and filtered. The solvent was removed under reduced pressure. Purification *via* flash chromatography (dichloromethane/ethyl acetate = 20:1) afforded **4** as a white solid (6.59 g, 90%). Non-symmetric pillar[5]arene **4** has four constitutional isomers **4a**, **4b**, **4c**, and **4d**. These four isomers could be separated with a molar ratio of 1:5:5:5, **4a** was separated lastly. The structure of **4a** could be determined since its proton NMR spectrum was analyzable.^{7h} The structures of other three isomers could not be determined since their spectra were complicated and their crystal structures were not obtained. The proton NMR spectrum of **4a** (mp 110.3–112.8 °C) is shown in Figure S1. ¹H NMR (400 MHz, acetone-*d*₆, 298 K) δ (ppm): 8.16 (s, 5H), 7.74–7.68 (m, 20H), 7.42–7.39 (m, 10H), 7.32 (d, *J* = 8.0 Hz, 5H), 6.96 (s, 5H), 6.88 (s, 5H), 5.62 (s, 10H), 4.82 (s, 10H), 3.70 (d, *J* = 8.0 Hz, 15H), 2.82 (s, 10H). The ¹³C NMR spectrum of **4a** is shown in Figure S2. ¹³C NMR (125 MHz, acetone-*d*₆, 298 K) δ (ppm): 205.43, 150.81, 149.31, 144.48, 133.53, 133.32, 133.05, 128.62, 128.25, 127.94, 127.66, 127.08, 126.43, 126.33, 125.58, 123.92, 115.25, 113.37, 62.08, 55.07, 53.48, 29.46, 29.30, 29.15, 28.99, 28.84, 28.69, 28.53.. LRESIMS is shown in Figure S3: *m/z* 1787.2 [M+H]⁺ (100%). HRESIMS: *m/z* calcd for [M + H]⁺ C₁₁₀H₉₅N₁₅O₁₀, 1787.7476, found 1787.7516, error 2.2 ppm.

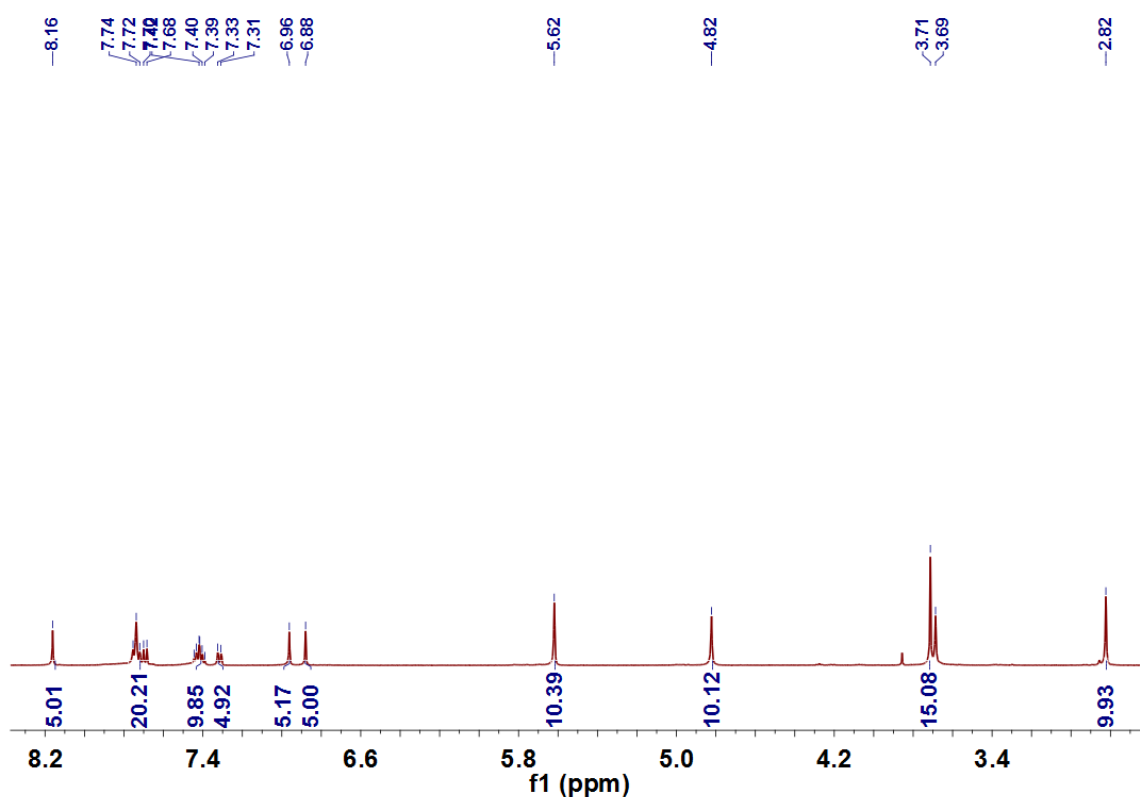


Figure S1. ¹H NMR spectrum (400 MHz, acetone-*d*₆, 298 K) of **4a**.

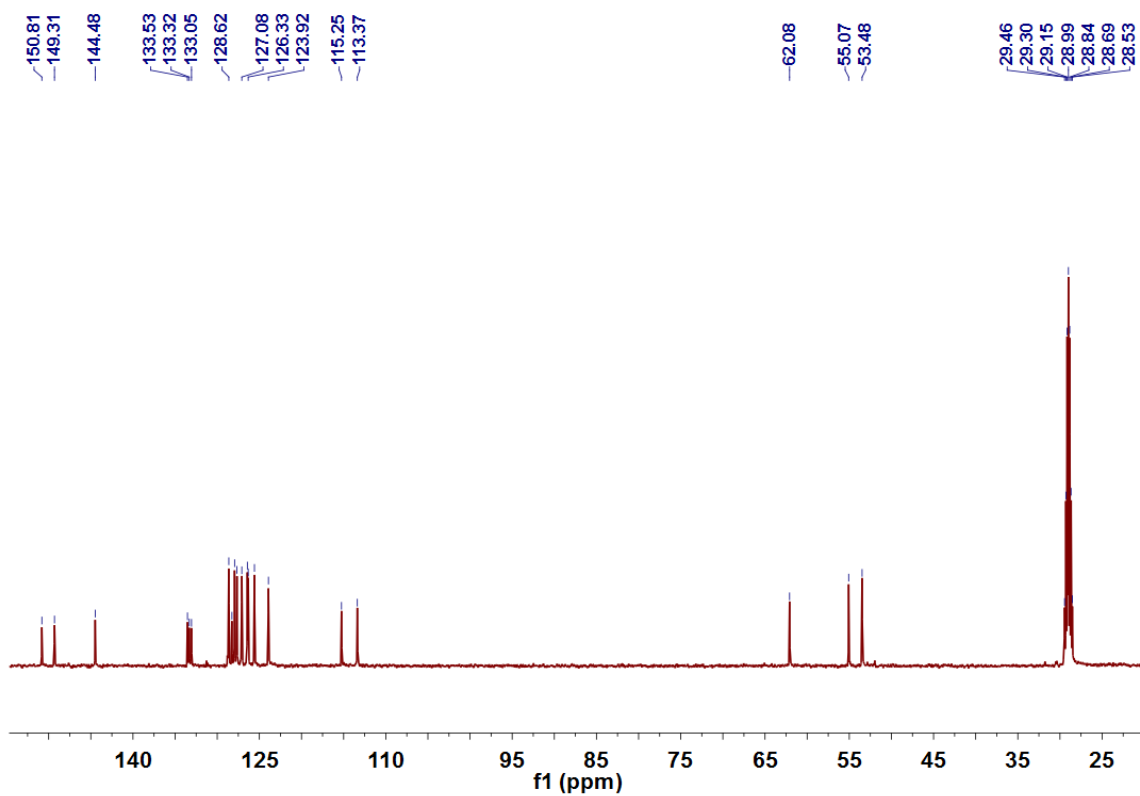


Figure S2. ^{13}C NMR spectrum (125 MHz, acetone- d_6 , 298 K) of **4a**.

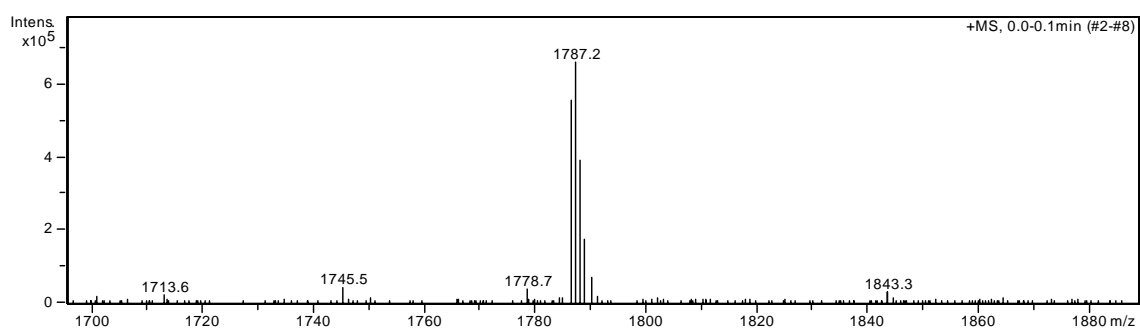
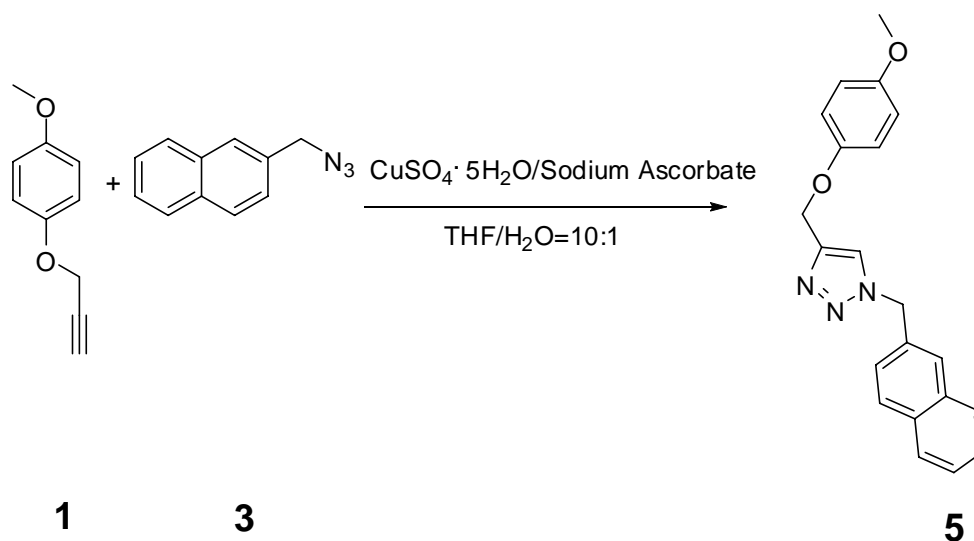


Figure S3. Electrospray ionization mass spectrum of **4a**. Assignment of the main peak: m/z 1787.2 $[\text{M} + \text{H}]^+$ (100%).



A solution of **1** (1.62 g, 10.0 mmol), **3** (1.86 g, 10.0 mmol), $\text{CuSO}_4 \cdot 5\text{H}_2\text{O}$ (0.250 g, 1.00 mmol), and sodium ascorbate (0.860 g, 5.00 mmol) in THF/ H_2O (50 mL/5 mL) was stirred at room temperature under nitrogen atmosphere for 24 h. The solvents were removed. The residue was subjected to silica gel chromatography (ethyl acetate/dichloromethane = 1:4) to afford the product as a white solid (3.20 g, 92%), mp 116.3–118.8 °C. ^1H NMR (400 MHz, chloroform-*d*, 298 K) δ (ppm): 8.09 (s, 1H), 7.93–7.87 (m, 4H), 7.54–7.46 (m, 3H), 6.95–6.92 (m, 2H), 6.85–6.82 (m, 2H), 5.81 (s, 2H), 5.10 (s, 2H), 3.72 (s, 3H) (Figure S7). The ^{13}C NMR spectrum of **5** is shown in Figure S8. ^{13}C NMR (125 MHz, chloroform-*d*, 298 K) δ (ppm): 154.41, 152.53, 133.44, 132.05, 129.45, 128.19, 128.04, 127.70, 127.01, 125.60, 122.94, 116.10, 114.87, 63.05, 55.92, 54.70. LRESIMS is shown in Figure S9: m/z 346.1 $[\text{M} + \text{H}]^+$ (100%). HRESIMS: m/z calcd for $[\text{M}] \text{C}_{21}\text{H}_{19}\text{N}_3\text{O}_2$, 345.1477, found 345.1476, error 0.3 ppm

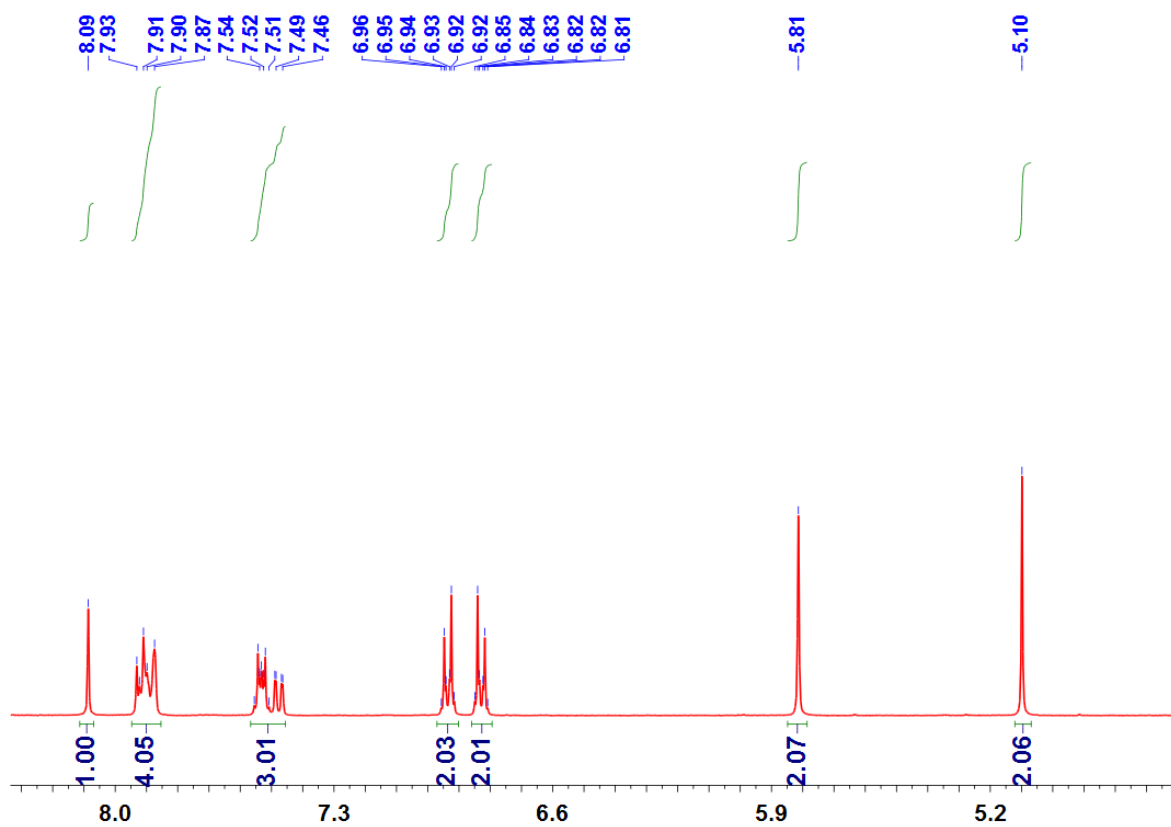


Figure S4. ^1H NMR spectrum (400 MHz, chloroform-*d*, 298 K) of **5**.

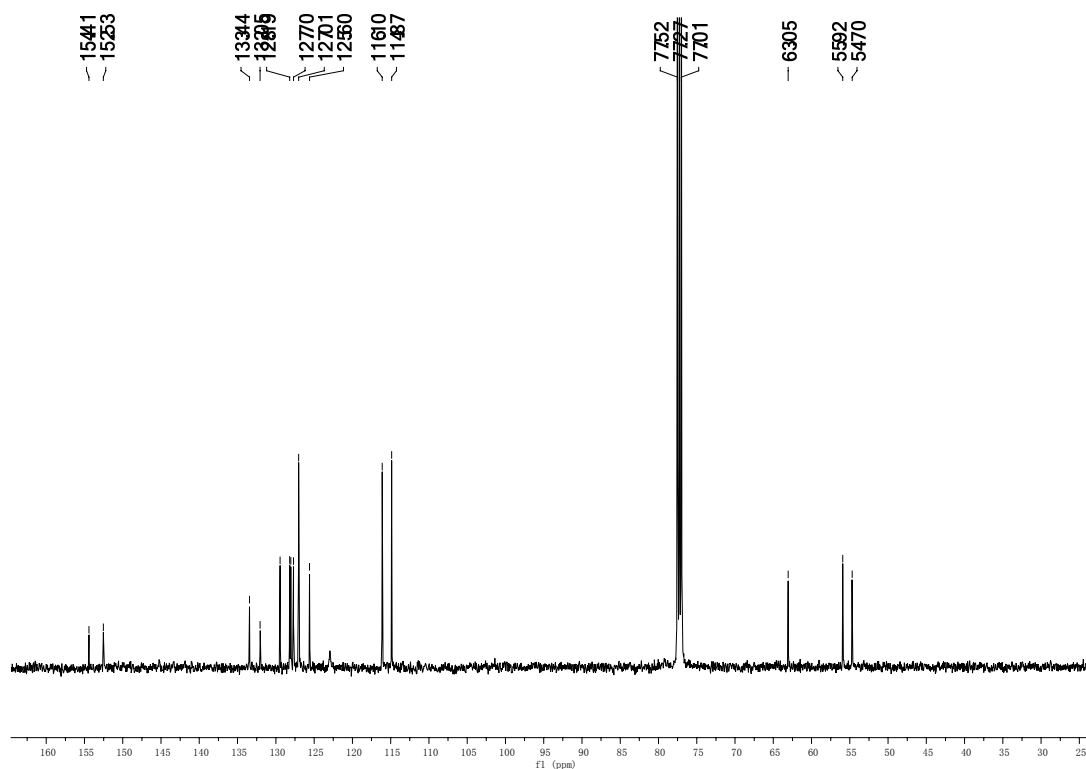


Figure S5. ^{13}C NMR spectrum (125 MHz, chloroform-*d*, 298 K) of **5**.

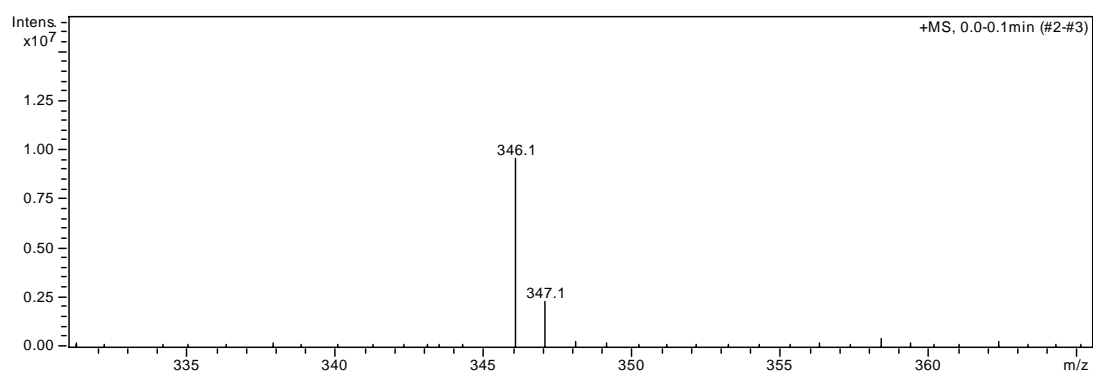


Figure S6. Electrospray ionization mass spectrum of **5**. Assignment of the main peak: m/z 346.1 $[M + H]^+$ (100%).

3. Determination of association constants for the complexes between **4a** and anions and between **5** and TBAF by fluorescence titration experiments

In the fluorescence titration experiments, the concentrations of the tetrabutylammonium salts were lower than 1.00 mM. According to literatures,^[S3] the salts could be thought to be completely dissociated, so the concentrations of the anions in the experiments were equal to the concentrations of the corresponding tetrabutylammonium salts.

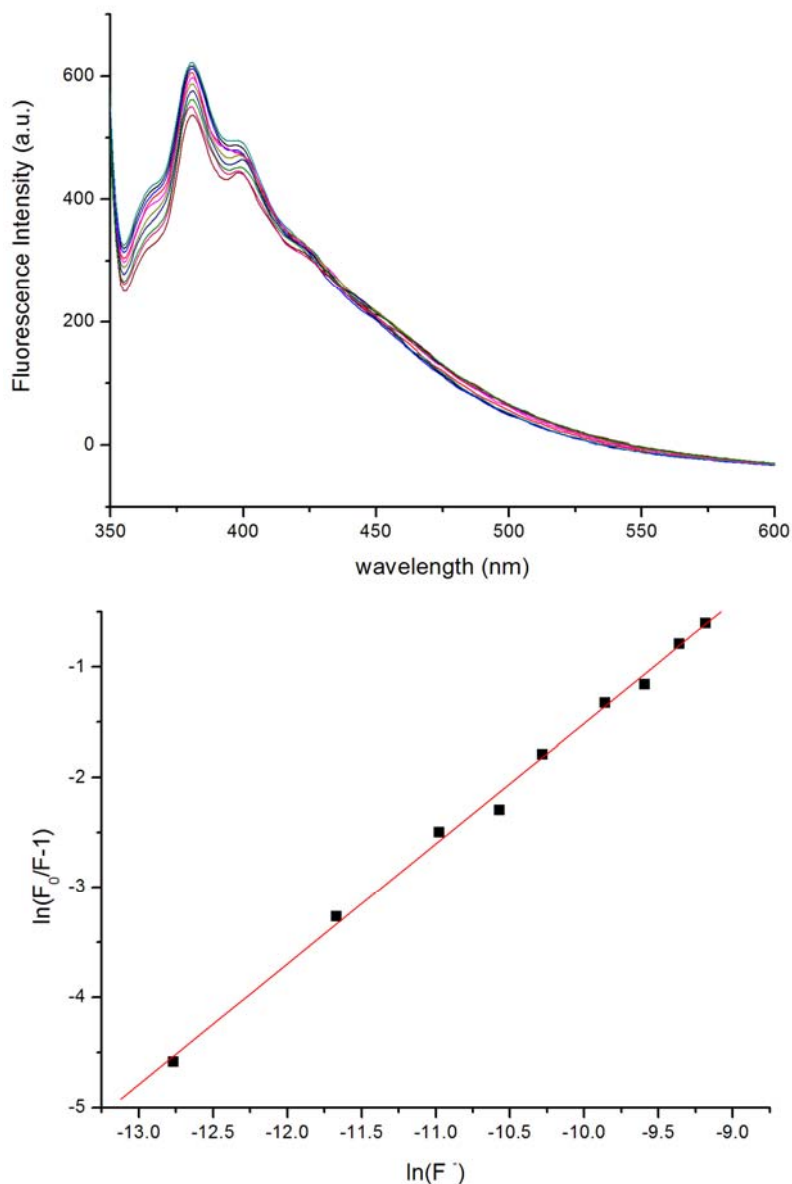


Figure S7. Fluorescence emission spectra of **4a** (1.50×10^{-4} M, $\lambda_{\text{ex}} = 340$ nm) in acetone at 298 K with different concentrations of F⁻ (from 0 to 9.00×10^{-4} M) (top) and the plot of the Stern-Volmer equation $\ln(F_0/F - 1) = \ln K + n \ln[F^-]$ for the complexation using the fluorimetric titration data at $\lambda_{\text{em}} = 381$ nm. F_0 is the initial fluorescent emission intensity of **4a** and F is the fluorescent emission intensity of **4a** in the presence of different concentrations of F⁻ (bottom).

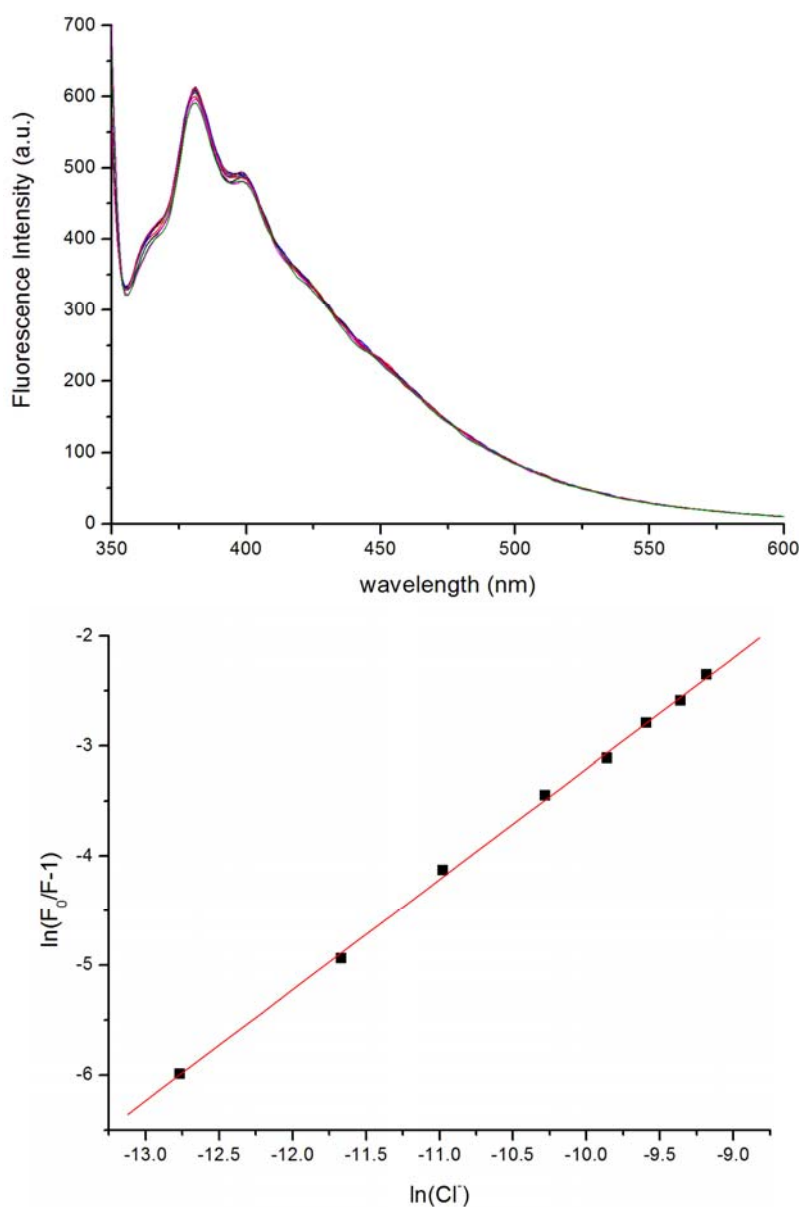


Figure S8. Fluorescence emission spectra of **4a** (1.50×10^{-4} M, $\lambda_{\text{ex}} = 340$ nm) in acetone at 298 K with different concentrations of Cl^- (from 0 to 9.00×10^{-4} M) (top) and the plot of the Stern-Volmer equation $\ln(F_0/F - 1) = \ln K + n \ln [\text{Cl}^-]$ for the complexation using the fluorimetric titration data at $\lambda_{\text{em}} = 381$ nm. F_0 is the initial fluorescent emission intensity of **4a** and F is the fluorescent emission intensity of **4a** in the presence of different concentrations of Cl^- (bottom).

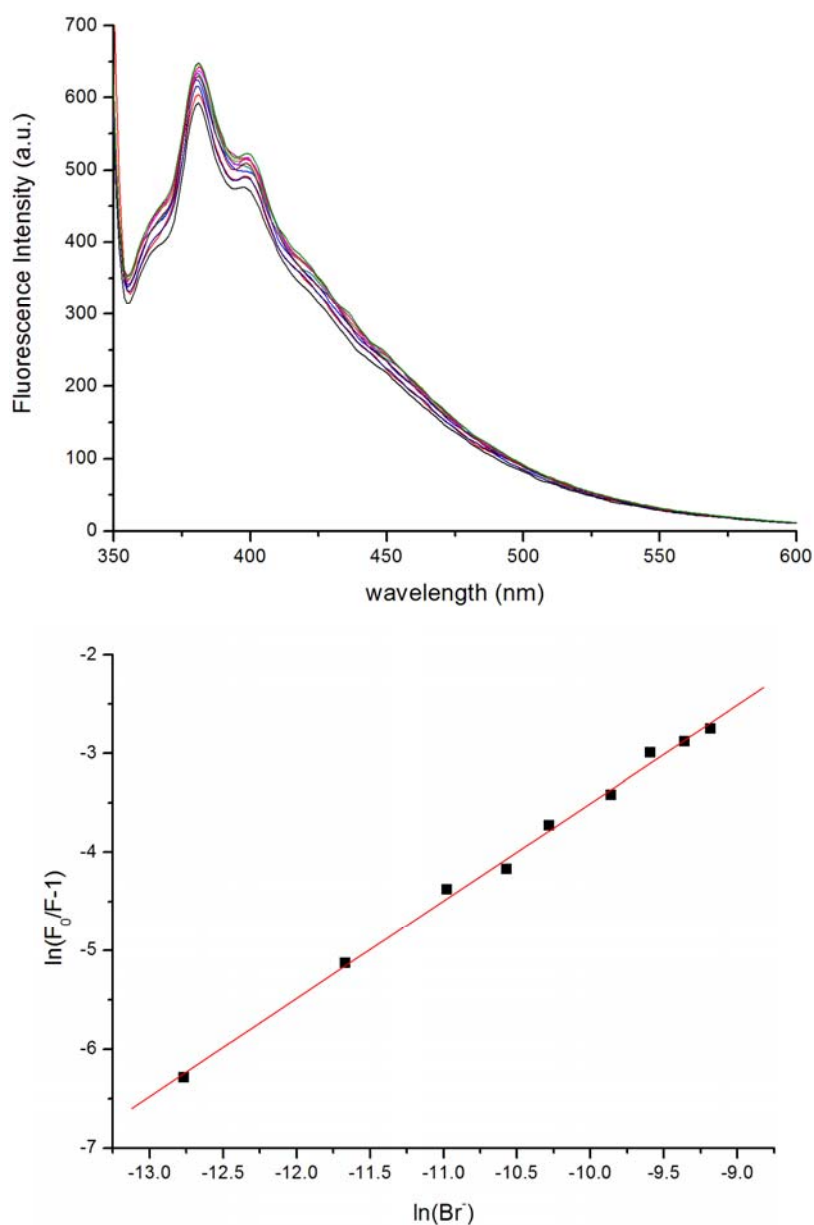


Figure S9. Fluorescence emission spectra of **4a** (1.50×10^{-4} M, $\lambda_{\text{ex}} = 340$ nm) in acetone at 298 K with different concentrations of Br⁻ (from 0 to 9.00×10^{-4} M) (top). The plot of the Stern-Volmer equation $\ln(F_0/F - 1) = \ln K + n \ln [\text{Br}^-]$ for the complexation using the fluorimetric titration data at $\lambda_{\text{em}} = 381$ nm. F_0 is the initial fluorescent emission intensity of **4a** and F is the fluorescent emission intensity of **4a** in the presence of different concentrations of Br⁻ (bottom).

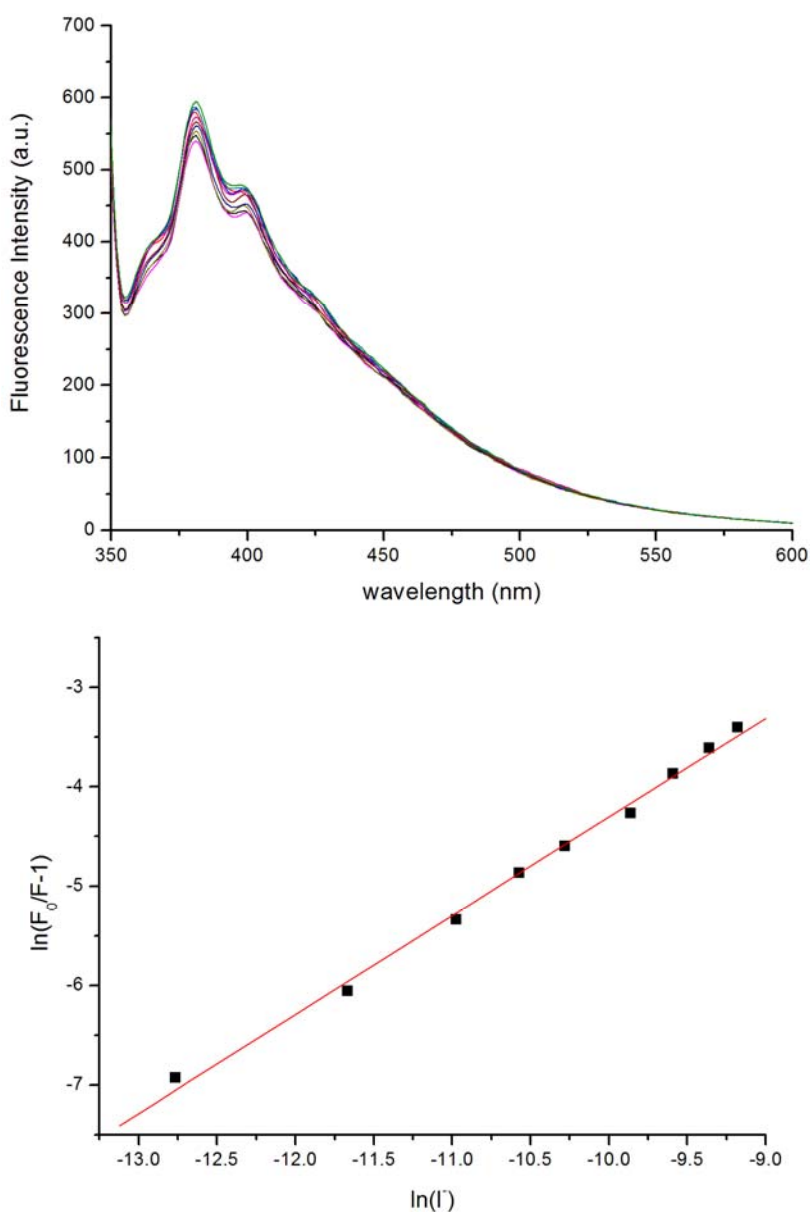


Figure S10. Fluorescence emission spectra of **4a** (1.50×10^{-4} M, $\lambda_{\text{ex}} = 340$ nm) in acetone at 298 K with different concentrations of Γ^- (from 0 to 9.00×10^{-4} M) (top) and the plot of the Stern-Volmer equation $\ln(F_0/F - 1) = \ln K + n \ln[\Gamma^-]$ for the complexation using the fluorimetric titration data at $\lambda_{\text{em}} = 381$ nm. F_0 is the initial fluorescent emission intensity of **4a** and F is the fluorescent emission intensity of **4a** in the presence of different concentrations of Γ^- (bottom).

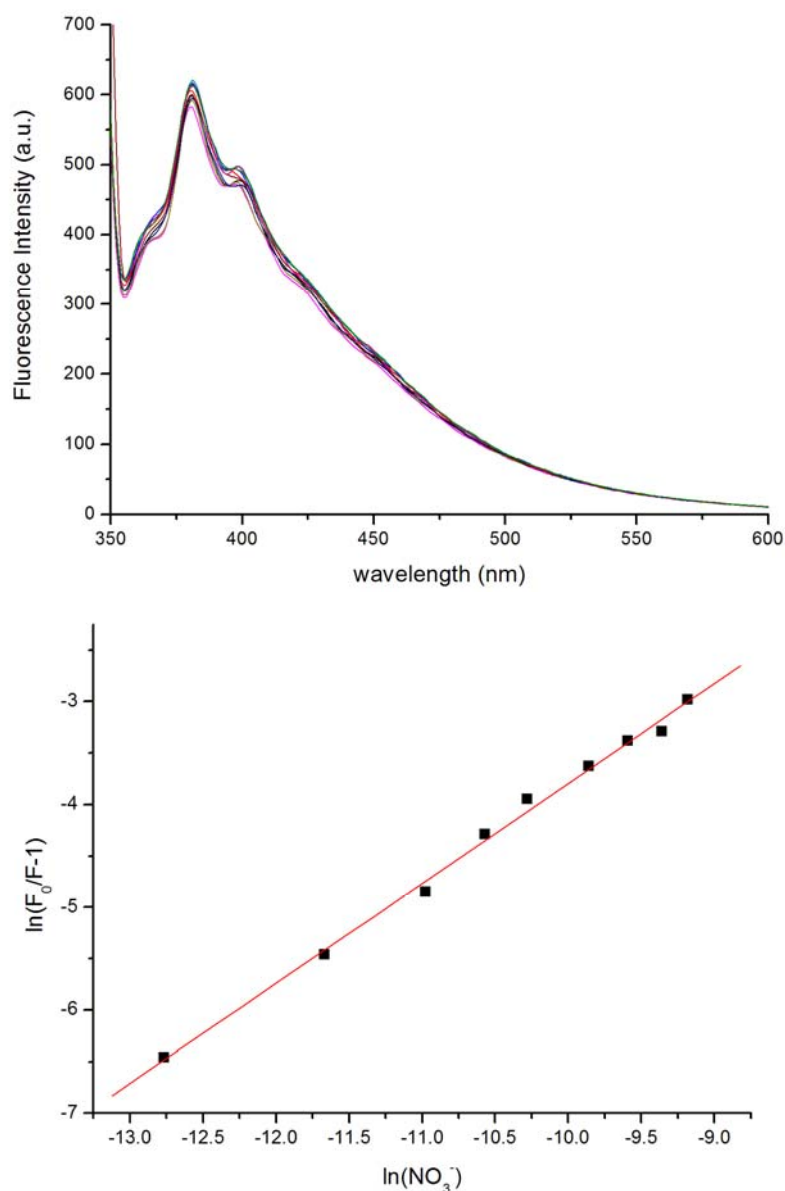


Figure S11. Fluorescence emission spectra of **4a** (1.50×10^{-4} M, $\lambda_{\text{ex}} = 340$ nm) in acetone at 298 K with different concentrations of NO_3^- (from 0 to 9.00×10^{-4} M) (top), and the plot of the Stern-Volmer equation $\ln(F_0/F - 1) = \ln K + n \ln[\text{NO}_3^-]$ for the complexation using the fluorimetric titration data at $\lambda_{\text{em}} = 381$ nm. F_0 is the initial fluorescent emission intensity of **4a** and F is the fluorescent emission intensity of **4a** in the presence of different concentrations of NO_3^- (bottom).

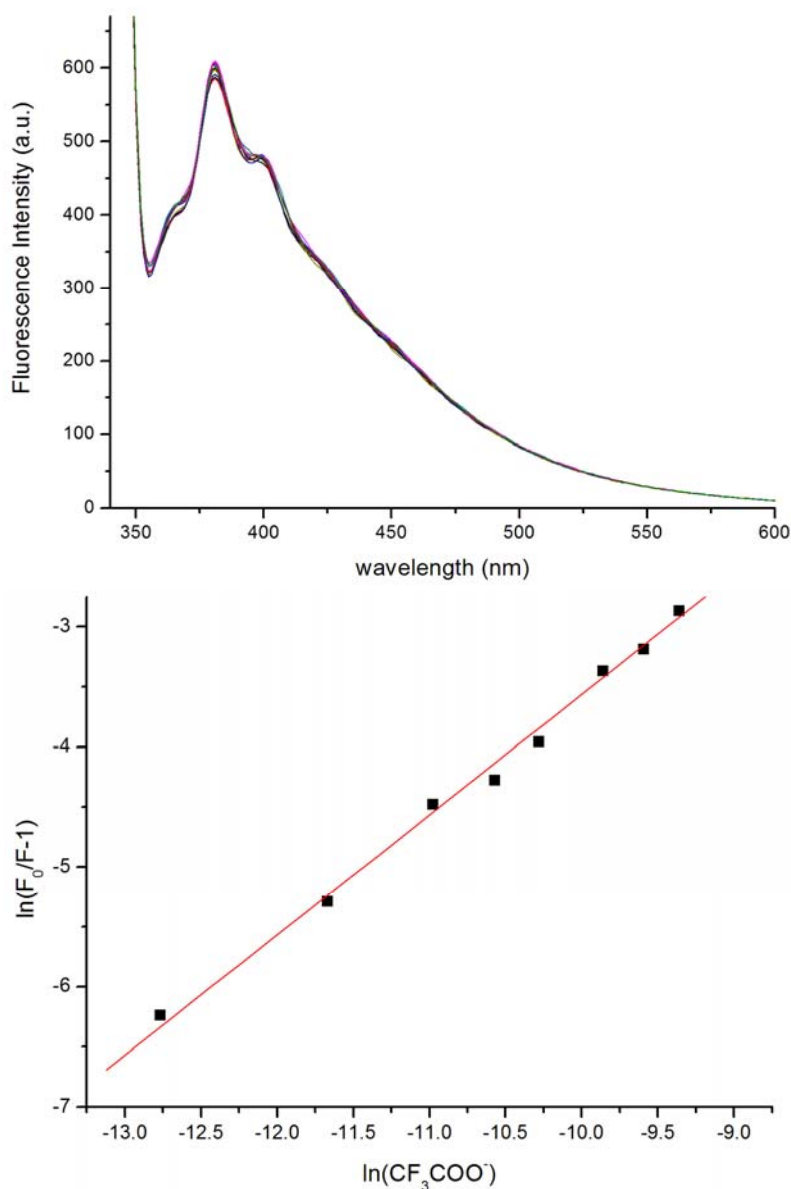


Figure S12. Fluorescence emission spectra of **4a** (1.50×10^{-4} M, $\lambda_{\text{ex}} = 340$ nm) in acetone at 298 K with different concentrations of CF_3COO^- (from 0 to 9.00×10^{-4} M) (top) and the plot of the Stern-Volmer equation $\ln(F_0/F - 1) = \ln K + n \ln[\text{CF}_3\text{COO}^-]$ for the complexation using the fluorimetric titration data at $\lambda_{\text{em}} = 381$ nm. F_0 is the initial fluorescent emission intensity of **4a** and F is the fluorescent emission intensity of **4a** in the presence of different concentrations of CF_3COO^- (bottom).

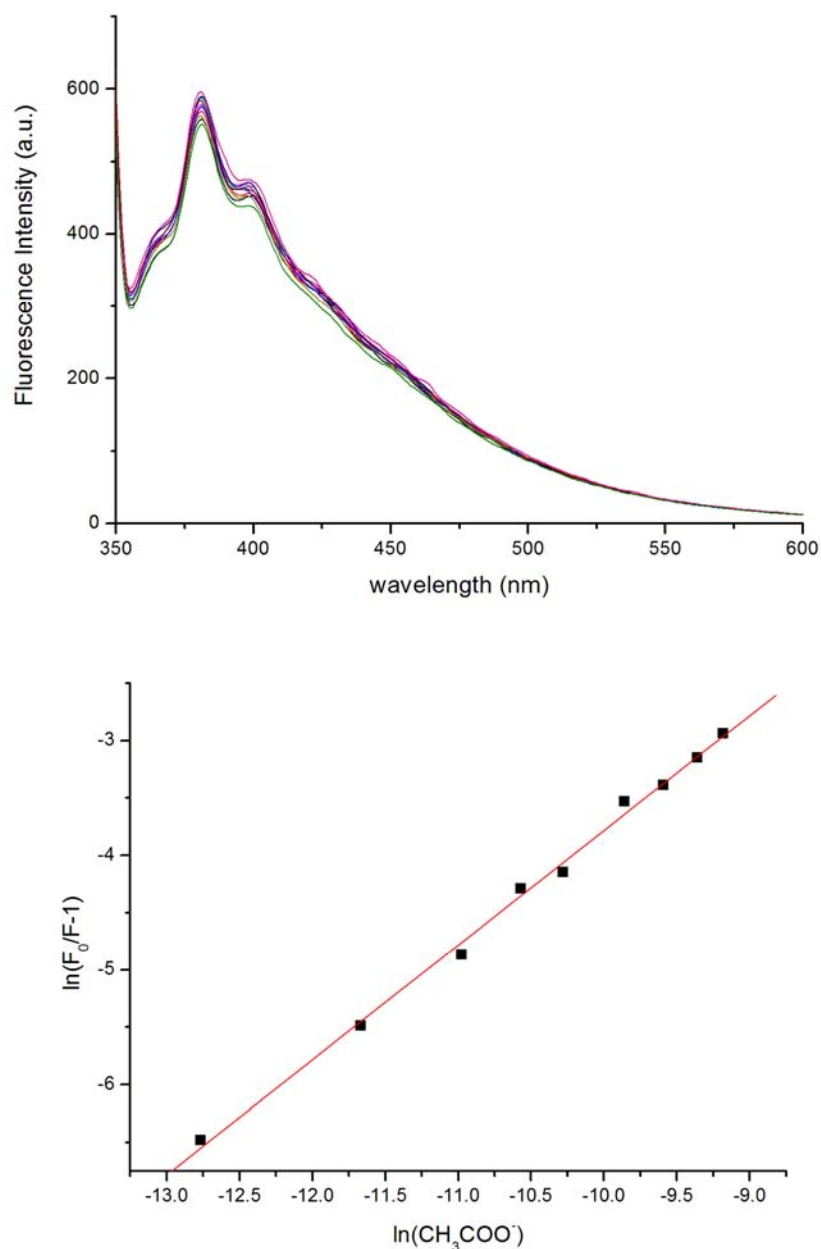


Figure S13. Fluorescence emission spectra of **4a** (1.50×10^{-4} M, $\lambda_{\text{ex}} = 340$ nm) in acetone at 298 K with different concentrations of CH_3COO^- (from 0 to 9.00×10^{-4} M) (top) and the plot of the Stern-Volmer equation $\ln(F_0/F - 1) = \ln K + n \ln[\text{CH}_3\text{COO}^-]$ for the complexation using the fluorimetric titration data at $\lambda_{\text{em}} = 381$ nm. F_0 is the initial fluorescent emission intensity of **4a** and F is the fluorescent emission intensity of **4a** in the presence of different concentrations of CH_3COO^- (bottom).

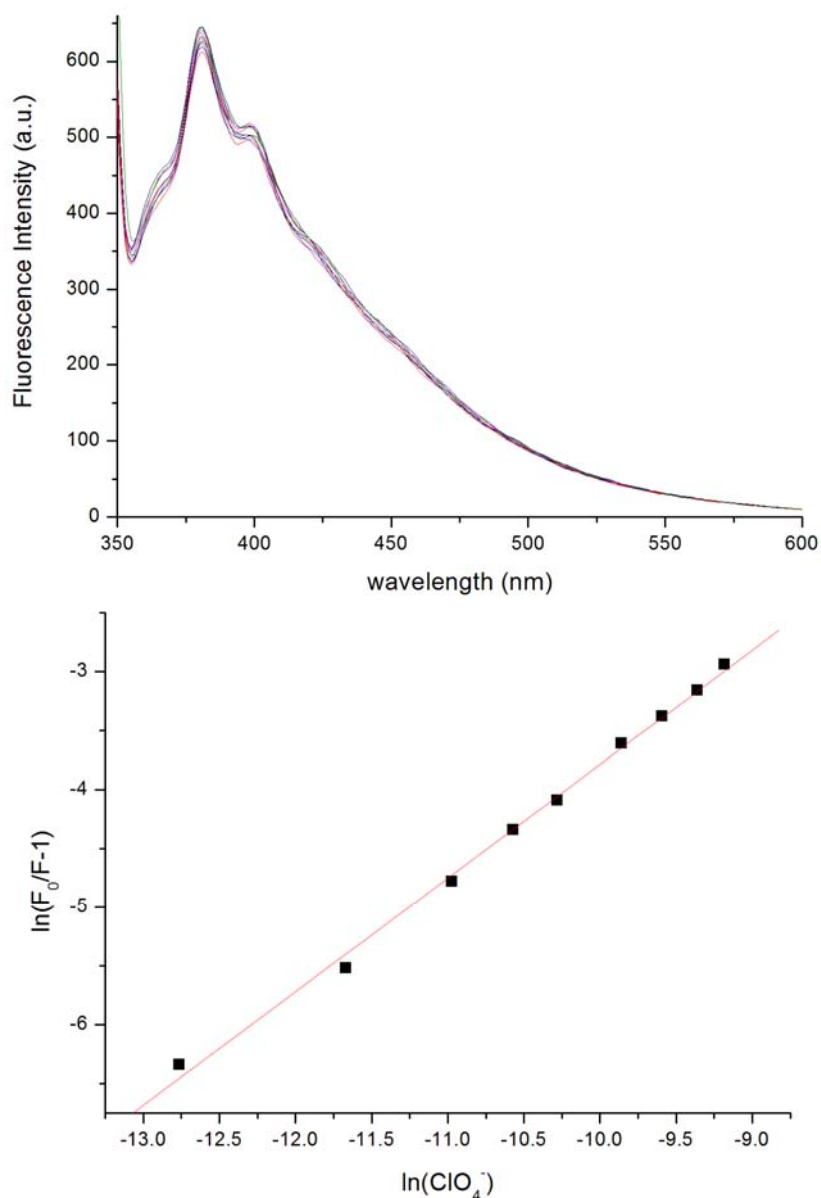


Figure S14. Fluorescence emission spectra of **4a** (1.50×10^{-4} M, $\lambda_{\text{ex}} = 340$ nm) in acetone at 298 K with different concentrations of ClO_4^- (from 0 to 9.00×10^{-4} M) (top) and the plot of the Stern-Volmer equation $\ln(F_0/F - 1) = \ln K + n \ln[\text{ClO}_4^-]$ for the complexation using fluorimetric titration data at $\lambda_{\text{em}} = 381$ nm. F_0 is the initial fluorescent emission intensity of **4a** and F is the fluorescent emission intensity of **4a** in the presence of different concentrations of ClO_4^- (bottom).

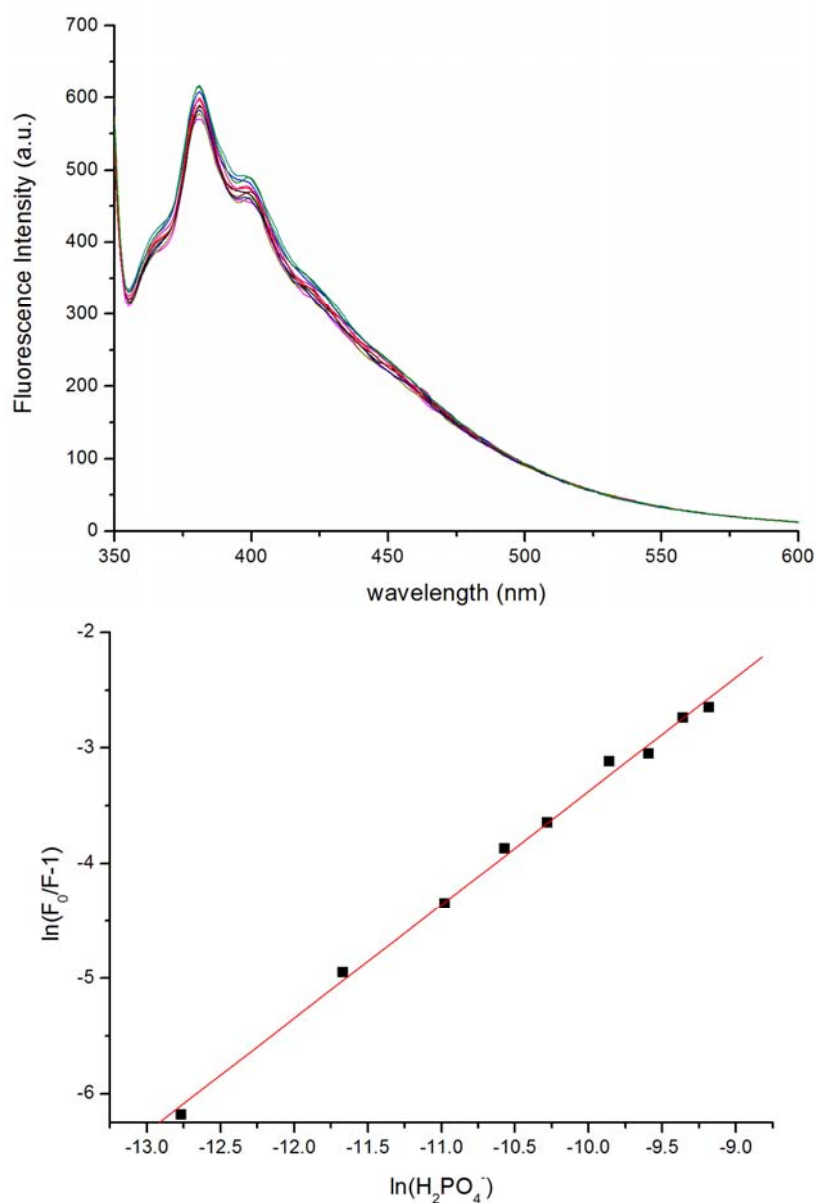


Figure S15. Fluorescence emission spectra of **4a** (1.50×10^{-4} M, $\lambda_{\text{ex}} = 340$ nm) in acetone at 298 K with different concentrations of H_2PO_4^- (from 0 to 9.00×10^{-4} M) (top) and the plot of the Stern-Volmer equation $\ln(F_0/F - 1) = \ln K + n \ln[\text{H}_2\text{PO}_4^-]$ for the complexation using fluorimetric titration data at $\lambda_{\text{em}} = 381$ nm. F_0 is the initial fluorescent emission intensity of **4a** and F is the fluorescent emission intensity of **4a** in the presence of different concentrations of H_2PO_4^- (bottom).

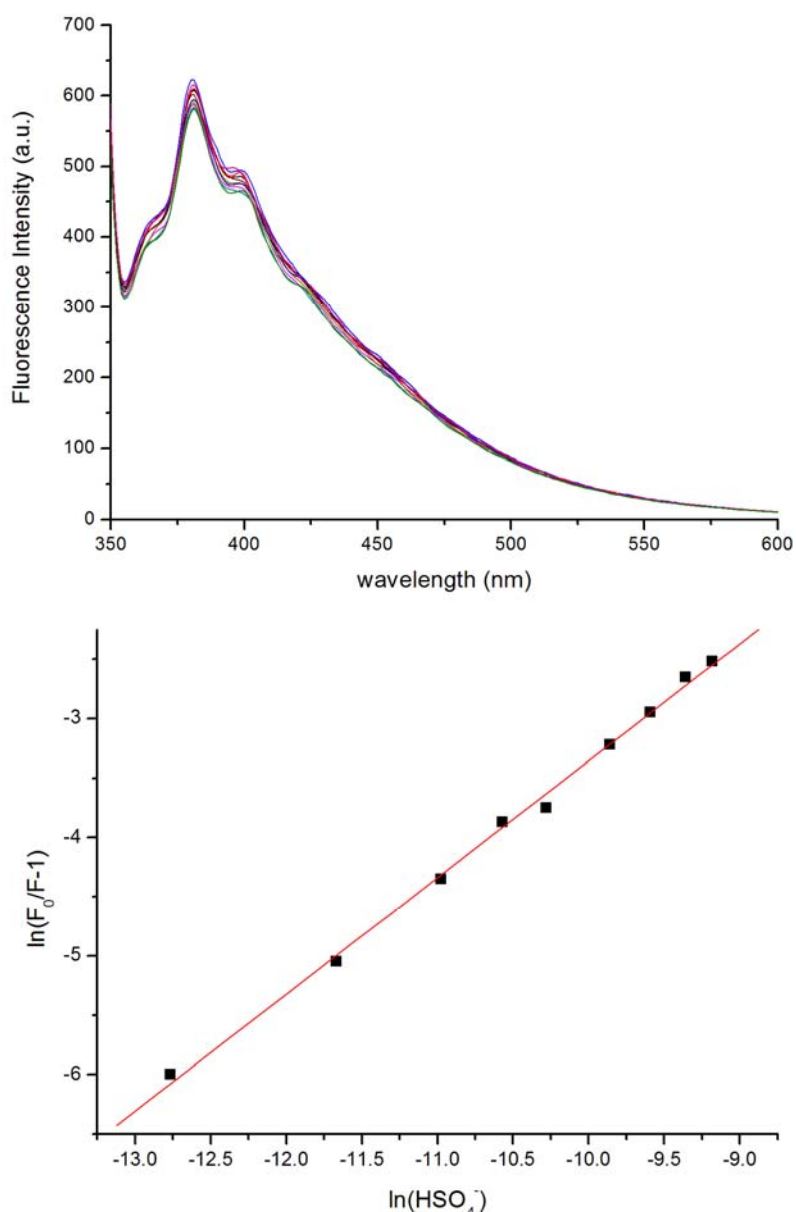


Figure S16. Fluorescence emission spectra of **4a** (1.50×10^{-4} M, $\lambda_{\text{ex}} = 340$ nm) in acetone at 298 K with different concentrations of HSO_4^- (from 0 to 9.00×10^{-4} M) (top) and the plot of the Stern-Volmer equation $\ln(F_0/F - 1) = \ln K + n \ln[\text{HSO}_4^-]$ for the complexation using fluorimetric titration data at $\lambda_{\text{em}} = 381$ nm. F_0 is the initial fluorescent emission intensity of **4a** and F is the fluorescent emission intensity of **4a** in the presence of different concentrations of HSO_4^- (bottom).

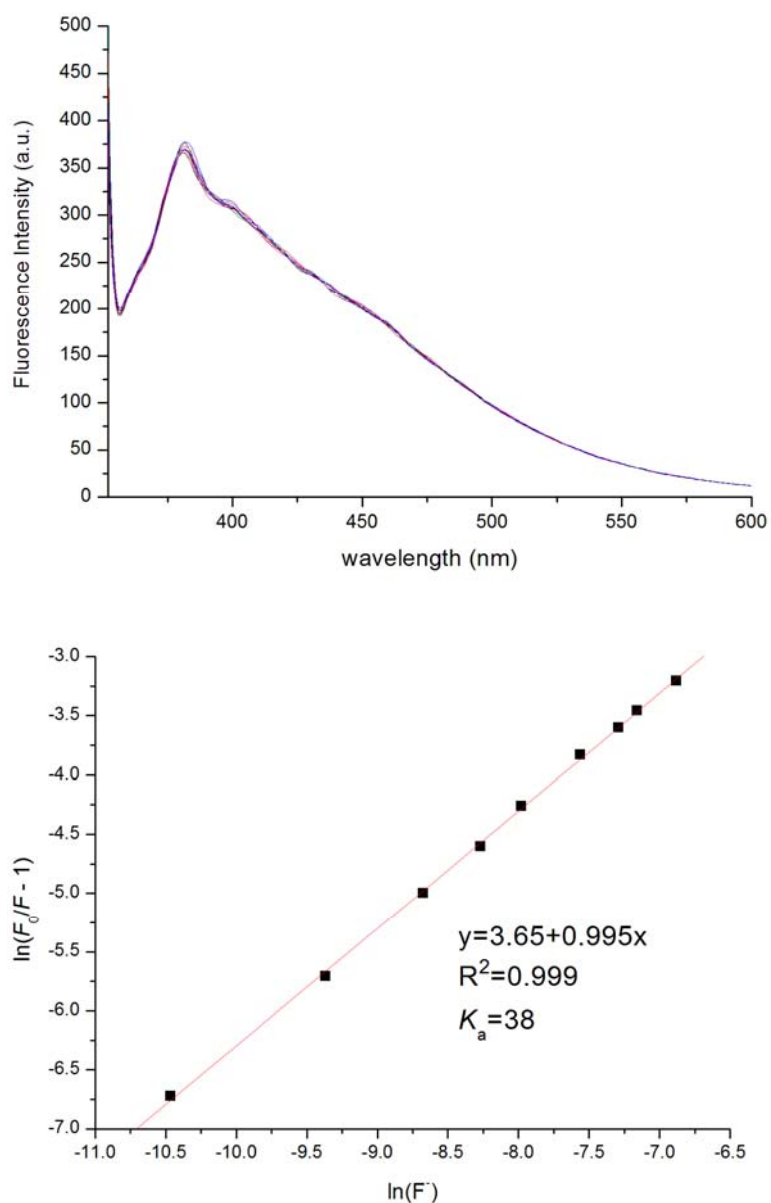


Figure S17. Fluorescence emission spectra of **5** (1.50×10^{-4} M, $\lambda_{\text{ex}} = 340$ nm) in acetone at 298 K with different concentrations of F^- (from 0 to 9.00×10^{-4} M) (top) and the plot of the Stern-Volmer equation $\ln(F_0/F - 1) = \ln K + n \ln[F^-]$ for the complexation using fluorimetric titration data at $\lambda_{\text{em}} = 379$ nm. F_0 is the initial fluorescent emission intensity of **5** and F is the fluorescent emission intensity of **5** in the presence of different concentrations of F^- (bottom).

4. Partial ^1H NMR spectra of model compound **5** and a mixture of **5** and tetrabutylammonium fluoride

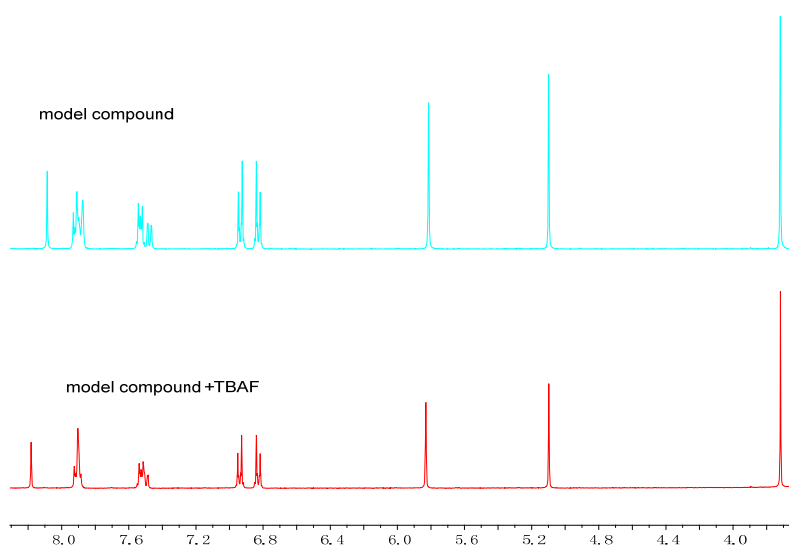


Figure S18. ^1H NMR spectrum (400 MHz, acetone- d_6 , 298 K) of **5** (top) and a mixture of **5** (1.00 mM) and tetrabutylammonium fluoride (4.00 mM) (bottom).

5. Partial ^1H NMR spectra recorded in acetone- d_6 during the titration of **4a** with TBAX

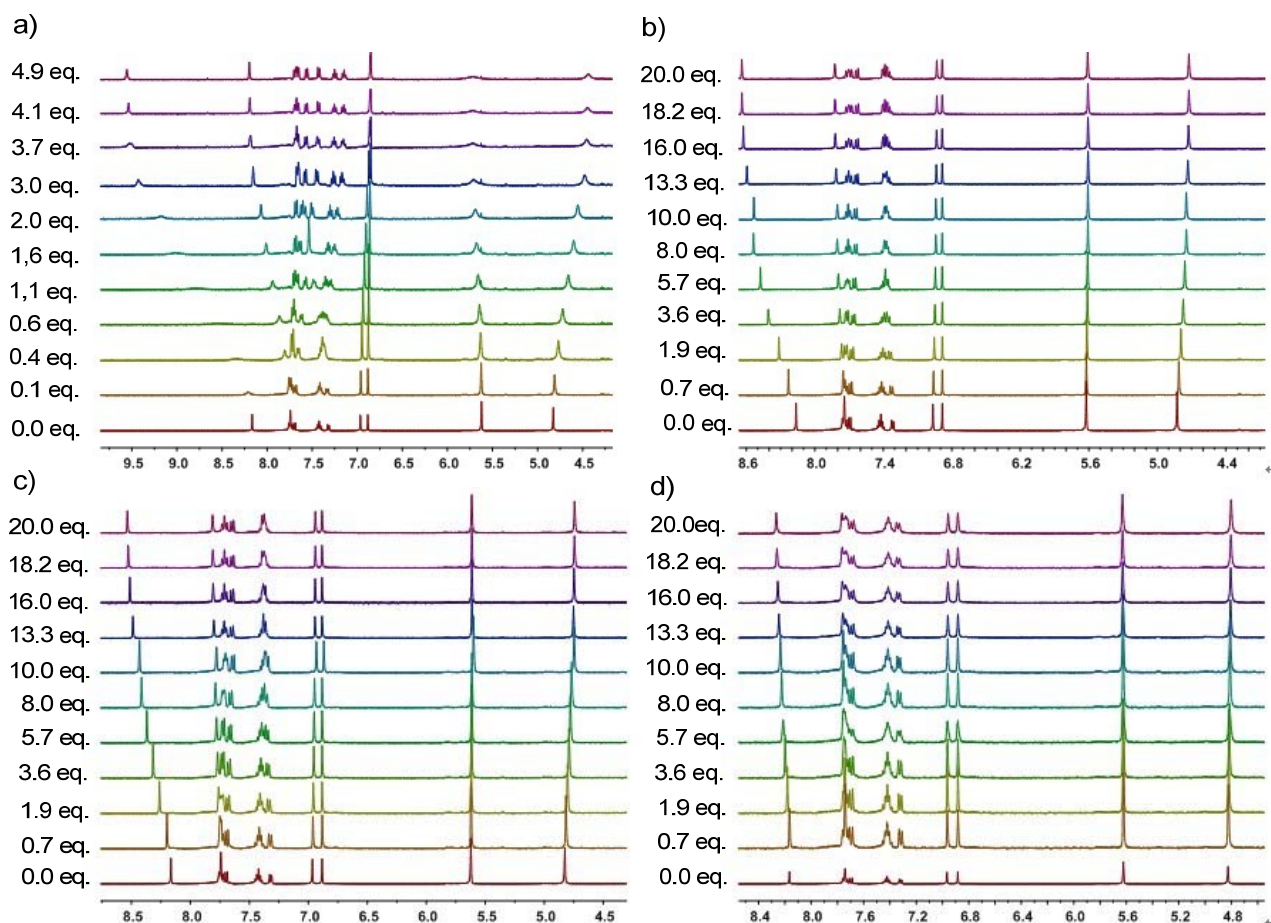


Figure S19. Partial ^1H NMR spectra of **4a** (1.00 mM) in acetone- d_6 at 298 K upon titration of (a) TBAF, (b) TBACl, (c) TBABr, and (d) TBAI.

6. ^{19}F NMR spectra of **4a** and a mixture of **4a** and tetrabutylammonium fluoride

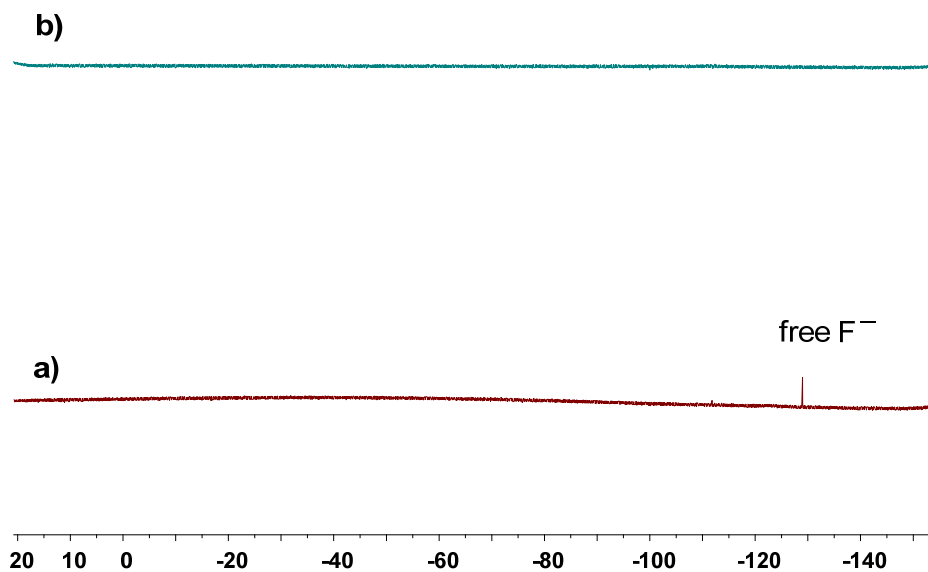


Figure S20. ^{19}F NMR spectra in acetone- d_6 at 298 K: a) TBAF (2.00 mM); b) an equimolar mixture of **4a** and TBAF (2.00 mM).

7. ^1H - ^1H NOESY spectra of **4a** and **4a** in the presence of 2 equiv of TBAF in acetone- d_6 at 298 K

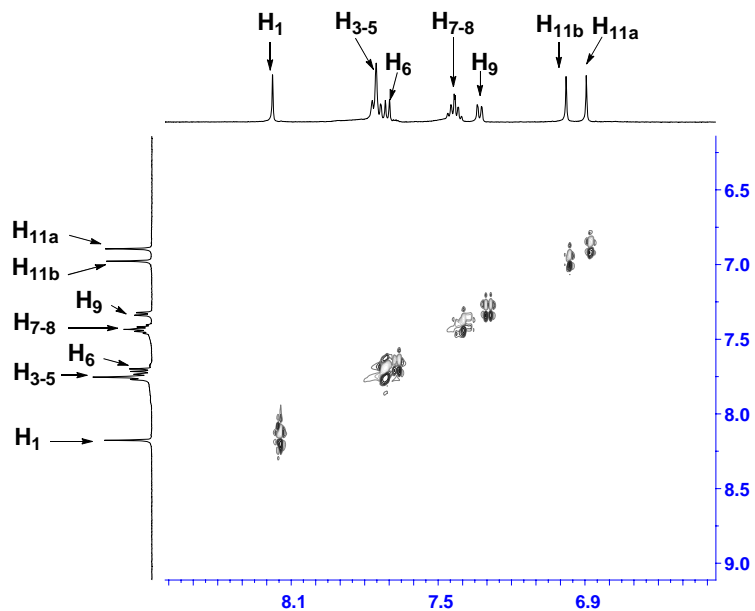


Figure 21. 2D ^1H - ^1H NOESY spectrum of **4a** in acetone- d_6 at 298 K.

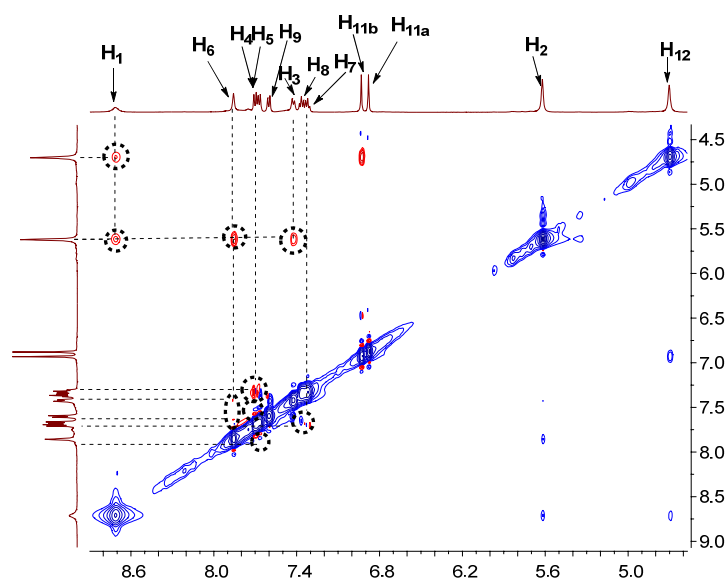


Figure 22. 2D ^1H - ^1H NOESY spectrum of **4a** in acetone- d_6 at 298 K after addition of 2 equiv of TBAF.

8. Partial ^1H NMR spectra of mixtures of **4a** and tetrabutylammonium salts with different anions

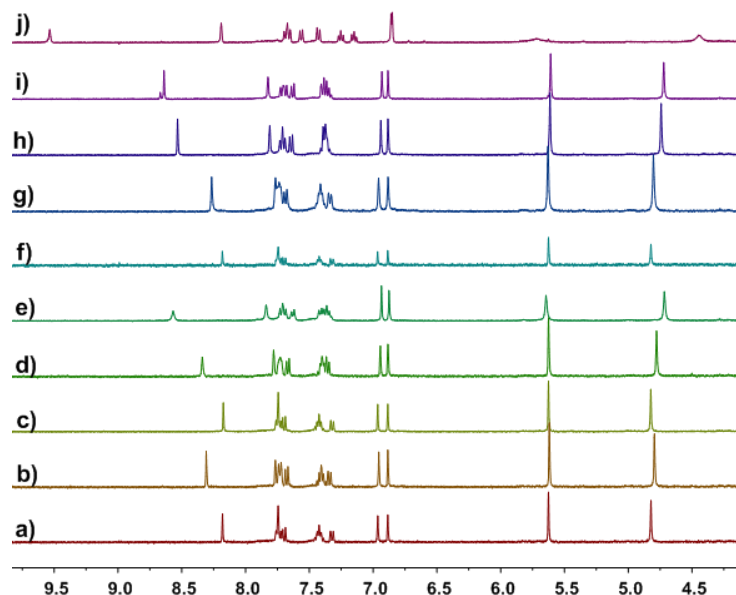


Figure S23. Partial ^1H NMR spectra (400 MHz, acetone- d_6 , 298 K): a) **4a** (1.00 mM) and 4 equiv of TBACF₃COO; b) **4a** (1.00 mM) and 4 equiv of TBACH₃COO; c) **4a** (1.00 mM) and 4 equiv of TBAClO₄; d) **4a** (1.00 mM) and 4 equiv of TBAH₂PO₄; e) **4a** (1.00 mM) and 4 equiv of TBAHSO₄; f) **4a** (1.00 mM) and 4 equiv of TBANO₃; g) **4a** (1.00 mM) and 4 equiv of TBAI; h) **4a** (1.00 mM) and 4 equiv of TBABr; i) **4a** (1.00 mM) and 4 equiv of TBACl; j) **4a** (1.00 mM) and 4 equiv of TBAF.

Table S1. Association constants (K_a) and stoichiometries (n) for the complexes between **4a** and different anions (the common cation is tetrabutylammonium) determined by fluorescence titration experiments

Anions	F	Cl	Br	I	NO ₃	PF ₆
K_a	$(1.25 \pm 0.08) \times 10^4$	858 ± 73	614 ± 51	284 ± 19	351 ± 22	/
n	1.09 ± 0.02	1.00 ± 0.01	0.99 ± 0.02	0.99 ± 0.03	0.98 ± 0.02	/
Anions	CF ₃ COO	CH ₃ COO	ClO ₄	H ₂ PO ₄	HSO ₄	
K_a	637 ± 47	473 ± 26	318 ± 19	576 ± 38	624 ± 54	
n	1.00 ± 0.03	1.00 ± 0.02	0.97 ± 0.02	0.99 ± 0.02	0.98 ± 0.02	

The addition of PF₆⁻ into the solution of **4a** showed no changes in the fluorescence spectra of **4a**. Furthermore, no chemical shift changes were observed on ¹H NMR spectra when 4 equiv of PF₆⁻ was added.

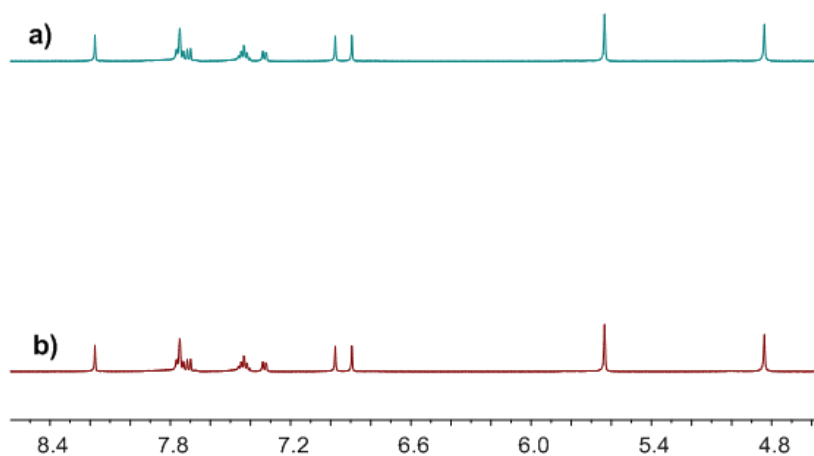


Figure S24. Partial ¹H NMR spectra (400 MHz, acetone-*d*₆, 298 K): a) **4a** (1.00 mM); b) **4a** (1.00 mM) and 4 equiv of TBAPF₆.

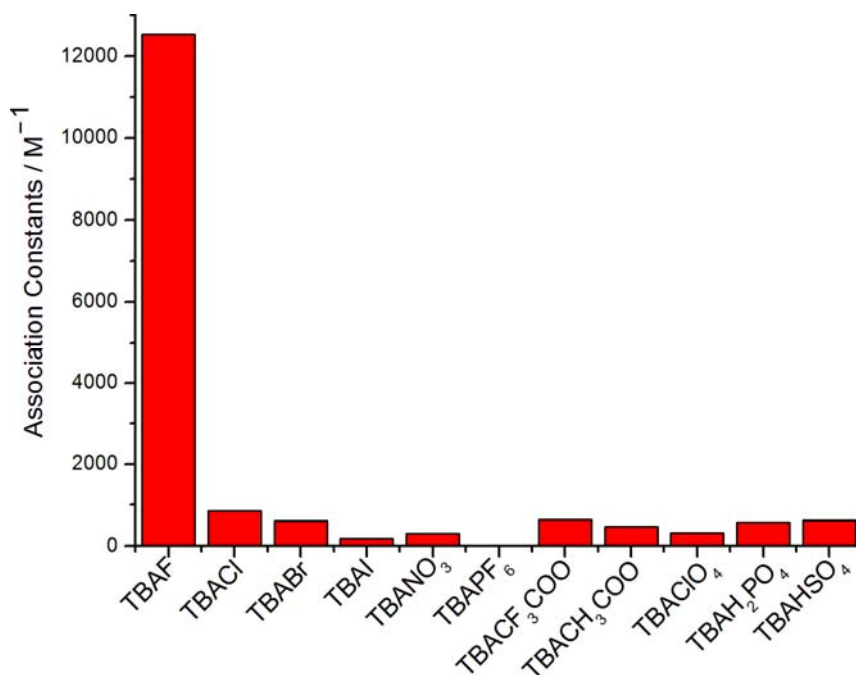


Figure S25. Association constants of fluorescent pillar[5]arene **4a** in the presence of different anions. The data were obtained through fluorescence titration experiments at 25 °C in acetone.

9. The energy-minimized structure of **4a** and **4a**⊃F⁻

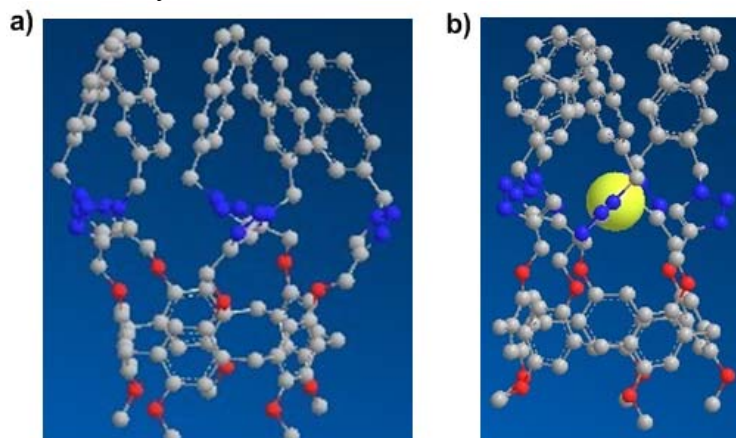


Figure S26. The energy-minimized structures of: (a) **4a**, (b) **4a**⊃F⁻. All hydrogen atoms have been omitted for clarity.

References:

- S1. M. Maddani and K. R. Prabhu, *Tetrahedron Lett.* 2008, **49**, 4526–4530.
- S2. M. E. Kopach, M. M. Murray, T. M. Braden, M. E. Kobierski and O. L. Williams, *Org. Process Res. Dev.* 2009, **13**, 152–160.
- S3 (a) P. L. Mercier and C. A. Kraus, *Proc. Natl. Acad. Sci. U. S. A.* 1956, **42**, 487–498. (b) S. Asai, H. Nakamura, M. Tanabe and K. Sakamoto, *Ind. Eng. Chem. Res.* 1993, **32**, 1438–1441. (c) H. Juwarker, J. M. Lenhardt, D. M. Pham and S. L. Craig, *Angew. Chem. Int. Ed.* 2008, **47**, 3740–3743.